Adsorbate-mediated relaxation dynamics of hot electrons at metal/organic interfaces

David Gerbert and Petra Tegeder*

Ruprecht-Karls-Universität Heidelberg, Physikalisch-Chemisches Institut, Im Neuenheimer Feld 253, 69120 Heidelberg, Germany

(Received 13 June 2017; revised manuscript received 21 September 2017; published 11 October 2017)

Hot-electron dynamics at metal surfaces are crucial for charge transport properties and chemical reactions at metal/organic interfaces. In order to study the influence of electron-donating adsorbates on hot-electron lifetimes we performed femtosecond time-resolved two-photon photoemission measurements of tetrathiafulvalene (TTF)-covered Au(111) surfaces. The electron-donating nature of TTF provides density of states near the Fermi energy (E_F) increasing the possibility for electron-electron scattering events. This leads to an additional fast electron-electron scattering assisted hot-electron relaxation channel for low intermediate state energies ($E_i - E_F$) at the TTF/Au(111) interface with hot-electron lifetimes up to 340 fs. However, suppressing the electron donation via intercalation of electron-accepting tetracyanoquinodimethane molecules causes quenching of this fast electron relaxation channel. This results in an asymptotic increase of the hot-electron lifetimes for infinitesimal small intermediate state energies up to about 1000 fs as predicted by the pure Landau theory of Fermi liquids.

DOI: 10.1103/PhysRevB.96.144304

I. INTRODUCTION

The dynamics of optically excited electrons in metals are fundamental for the application of metal surfaces in (opto)electronic devices as the transient lifetime of (photo)excited hot electrons essentially determines charge transport properties and chemical reactions at metal/organic interfaces [1–9]. Thus, a detailed and qualitative knowledge about interfacial hot-electron relaxation phenomena is a prerequisite for technological engineering in solid-state physics and surface chemistry [5,9]. Generally, an enhanced probability of hot-electron participation in charge transport mechanisms or chemical reactions is the result of an increased hot-electron lifetime. The lifetime of (photo)excited hot electrons in noble metals is determined by the excitation energy, electronic band structure, spin polarization, dimensionality or film thickness, and sample morphology [10–16]. Consequently, possible contributing relaxation mechanisms might be scattering events with excited holes, other cold electrons [energetically located just below the Fermi energy (E_F)], phonons, plasmons, defects, or impurities, hot-electron diffusion, and the repopulation of lower excited states by secondary electrons [5,9,10,13]. Experimentally, at very low intermediate-state energies ($E_i - E_F$) [17], hot-electron lifetimes up to 600 fs were observed which makes time-resolved two-photon photoemission (TR-2PPE) an ideal experimental tool to study hot-electron lifetimes at metal surfaces as well as metal/organic interfaces.

For low excitation energies ($E_i - E_F < 0.5$ eV), several TR-2PPE studies have demonstrated that the relaxation dynamics of hot electrons at metal surfaces are dominated by inelastic electron-electron scattering [5,9,10]. Assuming a free-electron-like behavior, the Landau theory of Fermi liquids (FLT) describes the inelastic electron-electron scattering rate from which the lifetime of hot electrons (τ_{FLT}) can be calculated to $\tau_{FLT} = \tau_0 E_F^2/(E_i - E_F)^2$ [5,9,18]. Herein the prefactor τ_0 is principally determined by the hot-electron density and the lifetime of hot electrons strongly depends on the available phase space. Ergo, the hot-electron lifetimes tend to infinity for infinitesimal small intermediate-state energies as hot electrons can scatter only into lower-lying unoccupied electronic states. However, a significant deviation from FLT especially for small intermediate-state energies has been observed in experiments, which was assigned to a different secondary decay channel (see below) or a combination of additional decay channels. Conclusively, using a scaling factor z and a second (effective) decay constant τ_1, the lifetime of hot electrons τ can be implemented to the so-called applied FLT (aFLT) [13,19]:

$$\frac{1}{\tau} = \frac{1}{\tau_1} + \frac{1}{z\tau_{FLT}}. \quad (1)$$

This model adequately describes experimental data by Cao *et al.* [19] of ultrafast hot-electron dynamics in Au(111) films covered with a small amount of alkali metal atoms used to reduce the surface work function. They assigned the additional decay channel τ_1 to electron-phonon scattering with a corresponding upper lifetime limit of about 300 fs [19] by excluding hot-electron transport away from the surface. However, so far the influence of a very high scaling factor $z = 6.5$ used in the fitting procedure [19] and the electron donating alkali metal atoms are not clarified.

In this paper, we present a femtosecond TR-2PPE study on the hot-electron dynamics in tetrathiafulvalene (TTF)-covered Au(111) surfaces. TTF, a strong electron donating organic molecule, leads to an increase of the density of states near E_F due to hybridization between metal bands and molecular electronic states [20–22]. Interestingly, we were able to qualitatively reproduce the hot-electron lifetimes presented by Cao *et al.* for one to three monolayer (ML) TTF adsorbed on Au(111), but for a lower scaling factor ($z = 1.1$). At first glance, this suggests that the adsorption of TTF has no influence on the hot-electron dynamics. However, we find that intercalation of tetracyanoquinodimethane (TCNQ) molecules, a strong electron acceptor, into the TTF layer disturbs the well-defined interfacial electronic structure and strongly influences the hot-electron dynamics at the metal/organic interface. The electron dynamics show a diverging behavior for low intermediate-state energies from aFLT, while it can perfectly be described by FLT. Therefore we propose that for TTF/Au(111)

*Corresponding author: tegeder@uni-heidelberg.de

the well-defined interfacial electronic structure supports an additional, second relaxation channel for hot electrons, which can be associated to an adsorbate-induced increase of the interfacial density of occupied and unoccupied electronic states around E_F. Especially for very low intermediate state energies ($E_i - E_F < 0.3$ eV) this leads to an increased scattering rate, phase space, and conclusively to limited hot-electron lifetimes at the metal/organic interface.

II. METHODS

For sample preparation the Au(111) single crystal was cleaned by several sputtering (Ar^+, at room temperature) and annealing cycles (at 800 K, 30 min). TTF molecules were evaporated from an effusion cell held at 323 K and deposited on a Au(111) substrate at room temperature. The coverage was adjusted via the deposition time and monitored by temperature-programmed desorption (TPD). TCNQ was evaporated from an effusion cell held at 390 K and deposited onto the sample at room temperature. Sample preparation and TR-2PPE measurements were performed under ultrahigh vacuum conditions at a base pressure of 5.3×10^{-11} mbar. TR-2PPE measurements were performed at a sample temperature of around 90 K using femtosecond laser pulses of a 300 kHz Ti:sapphire laser system which pumps an optical parametric amplifier, giving a visible output with photon energies from 1.8 to 2.5 eV. Using a BBO crystal frequency doubling gives access to the ultraviolet photon energy range from 3.6 to 5.1 eV and the doubled fundamental beam resulting in a photon energy of 3.1 eV. With a first femtosecond laser pulse (pump pulse) electrons are excited from below E_F to an intermediate unoccupied electronic state below the vacuum level (E_{Vac}). A second photon (probe pulse) then lifts this formerly excited electron above E_{Vac} where its kinetic energy E_{kin} is measured using an electron time-of-flight (TOF) spectrometer [23]. In TR-2PPE measurements the probe pulse can be temporally delayed by varying the beam path which enables delay time tuning and time-resolved measurements [24–26]. Ultraviolet photoemission spectroscopy and energy-resolved 2PPE was used to study the electronic structure of the TTF/Au(111) interface as well as the mixed layer TCNQ/TTF on Au(111). 2PPE signals may arise from occupied or unoccupied electronic states, therefore photon energy-dependent measurements are needed for the assignment (for details, see Refs. [23,25,26]).

III. RESULTS AND DISCUSSION

Due to the limited photon energy range of existing 2PPE setups, hot-electron dynamics of a clean Au(111) surface have not been studied, since the work function of the bare Au(111) surface is 5.5 eV. This problem has been solved by lowering the work function using a small amount of adsorbed electron donating alkali metal atoms, which was assumed to have no influence on the hot-electron lifetime [19,27]. However in the present study, we utilized a different approach by depositing well-ordered molecular films of the electron donating organic semiconductor TTF on Au(111). Because of its electron donating nature, TTF adsorption lowers the Au(111) work function from 5.50 ± 0.02 to 4.15 ± 0.04 eV,

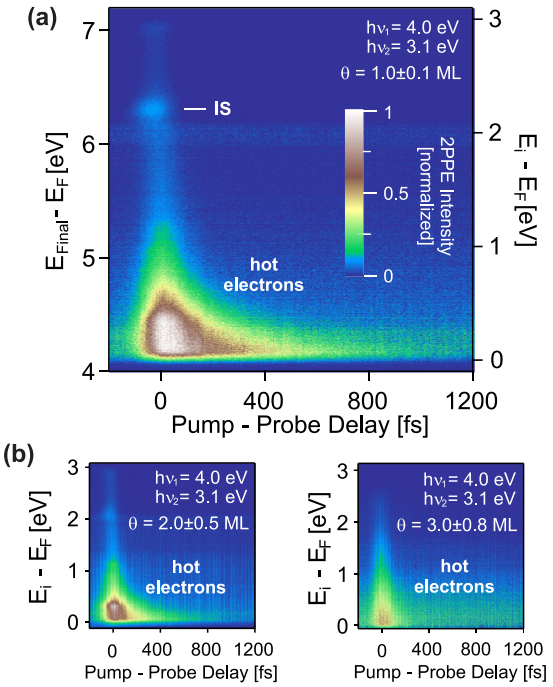

FIG. 1. TR-2PPE measurements of the TTF/Au(111) interface at different coverages. (a) At 1.0 ± 0.1 ML coverage hot electrons can be observed in an extended energy range of about 1 eV. Their lifetime increases up to some hundred femtoseconds for decreasing intermediate-state energy, whereas an unoccupied interfacial electronic state (IS) features no significant lifetime. (b) The adsorption of a second and third TTF layer has no significant influence on the hot-electron lifetimes but reduces the 2PPE signal intensity.

which enables us to study the hot-electron dynamics at the TTF/Au(111) interface using our TR-2PPE setup.

A. Coverage-dependent TR-2PPE data

Figure 1 displays three two-dimensional representations of TR-2PPE measurements for different TTF coverages taken at a pump energy of 3.1 eV and a probe energy of 4.0 eV. Such representations visualize the normalized correlated dichromatic 2PPE signal at a given final-state energy ($E_{Final} - E_F$) or intermediate-state energy ($E_i - E_F$) with respect to E_F as a function of pump-probe delay. Positive pump-probe delays imply that the probe pulse $h\nu_1$ reaches the sample after the pump pulse $h\nu_2$, and vice versa for negative delays. Figure 1(a) indicates that long-lived excited electrons can be found in the energetic region towards the secondary edge at $E_{Final} - E_F = 4.15 \pm 0.04$ eV or $E_i - E_F = 0.00 \pm 0.04$ eV, respectively, in an extended energy range of about 1 eV. In addition, it shows that for decreasing intermediate-state energy or phase space, respectively, the lifetime of these excited electrons rises. According to this behavior these long-lived photoexcited electrons can be assigned to hot electrons at the TTF/Au(111) interface. TR-2PPE measurements for higher coverages, shown in Fig. 1(b), illustrate that the 2PPE intensity near the secondary edge decreases but the lifetimes of the electrons are similar. This coverage dependency demonstrates that adsorption of more than one monolayer TTF has no significant impact on the hot-electron dynamics at the TTF/Au(111) interface.

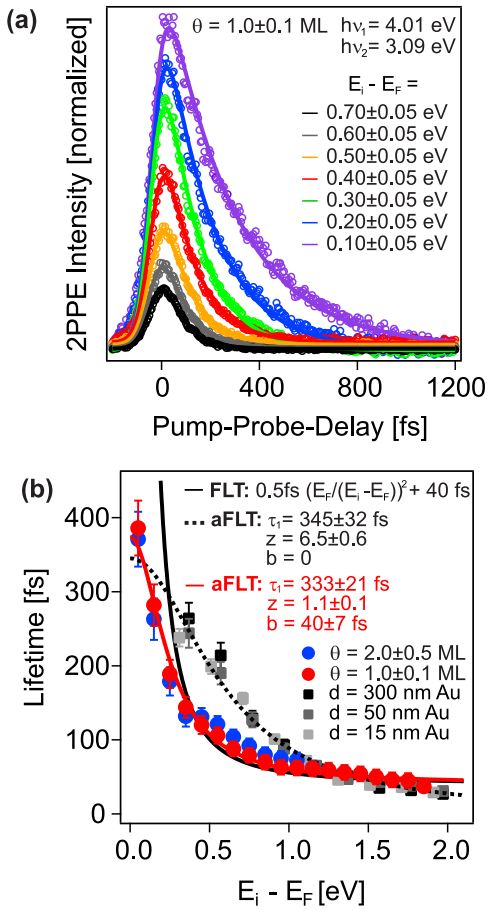

FIG. 2. Characterizing the hot-electron dynamics at the TTF/Au(111) interface. (a) Averaged XC curves for different intermediate-state energies fitted by a monoexponential decay function. (b) Energy-dependent hot-electron lifetimes for the TTF/Au(111) interfaces and alkali-metal-covered Au(111) films (data adopted from Ref. [19]).

A more detailed characterization of hot-electron dynamics at the TTF-covered Au(111) surface (coverage 1.0 ± 0.1 ML) is presented in Fig. 2. Figure 2(a) shows cross-correlation (XC) curves averaged for 0.1 eV intermediate-state energy ranges which were fitted using a monoexponential decay function. According to these fits, the hot-electron dynamics at the TTF/Au(111) surface can be described using one single exponential decay. Thereby the electron lifetimes significantly increase for decreasing intermediate-state energies. Figure 2(b) displays energy-dependent hot-electron lifetimes at the TTF/Au(111) interface for 1.0 ± 0.1 and 2.0 ± 0.5 ML, respectively. For comparison, the hot-electron lifetimes in Au(111) films covered with alkali metal atoms provided by Cao *et al.* [19] are included. For high intermediate-state energies ($E_i - E_F > 1.0$ eV) the dynamics at the TTF/Au(111) interface and in thin Au(111) films coincide, whereas for low intermediate-state energies significant differences occur. The hot-electron dynamics at the TTF/Au(111) interface are characterized by a steeper lifetime increase up to almost 400 fs in comparison to the respective lifetimes in Au(111) films which includes shorter lifetimes in the range from 0.3 to 1.0 eV. It has been shown that in particular for Au not only diffusive transport but also ballistic transport of hot electrons have to be considered [9,28,29]. Additionally, differences between the dynamics in the bulk and thin films have been found in the case of Ag, which has been attributed to different transport properties [9]. Thus, the shorter lifetimes found here for TTF/Au(111) may be related to transport effects. The dynamics at the TTF/Au(111) interface above $E_{\mathrm{Final}} - E_F = 0.4$ eV can be adequately described using the FLT model and a constant background b. Including a scaling factor z and an additional decay constant τ_1 also the region below 0.4 eV can be sufficiently modeled as it was previously done by Cao *et al.* [19]. The observed FLT-like behavior above 0.4-eV intermediate-state energy and the low scaling factor close to 1 serve as an argument for the high quality of the TTF/Au(111) interface. From the applied FLT fit (aFLT) the additional decay constant τ_1 can be estimated to amount to 333 ± 21 fs, which is consistent with the respective decay constant in alkali-metal-covered single-crystal Au(111) films [19]. At first glance, this consistence constitutes a sufficient reason to assign this additional decay channel to electron-phonon scattering (see below). In principle, electron-phonon scattering *per se* should not be influenced by the interfacial electronic structure because phonon excitations are a solid-state phenomenon. On the other hand electron-adsorbate phonon scattering at the TTF/Au(111) interface could play a role as a decay channel for the hot electrons [30,31].

The presented results suggest a negligible impact of TTF adsorption on hot-electron dynamics in Au(111), in full agreement with the electron-phonon scattering interpretation. However, the adsorption of electron donating molecules on the Au(111) surface induces additional electronic states around E_F [see Fig. 3(a)], which should influence the hot-electron lifetimes at metal surfaces as they increase the phase space and the concentration of electrons as scattering partners directly at the interface [32–34]. Figure 3(a) shows ultraviolet photoemission spectroscopy (UPS) data of the bare and the TTF-covered Au(111) surface. For the bare surface the Shockley surface state (SS) is observed, which is quenched at a TTF coverage of 1 ML. Moreover, a new peak labeled HOMO* just below the Fermi edge is observed. According to density functional theory (DFT) results this spectral feature can be assigned to a hybridized interfacial electronic state derived from the Au(111) surface state and the highest occupied molecular orbital (HOMO) of TTF [20,35]. Further occupied electronic states are located at -1.2 and -1.6 eV. They are attributed to the HOMO and HOMO-1, respectively. However, we expect an impact of the hybridization between metallic and molecular states at the TTF/Au(111) interface [20–22] on the hot-electron dynamics.

B. TCNQ intercalation

In order to elucidate the influence of the electronic structure at the TTF/Au(111) interface, we introduced TCNQ molecules into the TTF monolayer to disturb the hybridization at the TTF/Au(111) interface. TCNQ molecules have been deposited on top of the TTF/Au(111) interface at full monolayer coverage which was held at liquid-nitrogen temperature. Since adsorption of TCNQ increases the work function (see below) due to its strong electron-accepting nature (high electron affinity) the

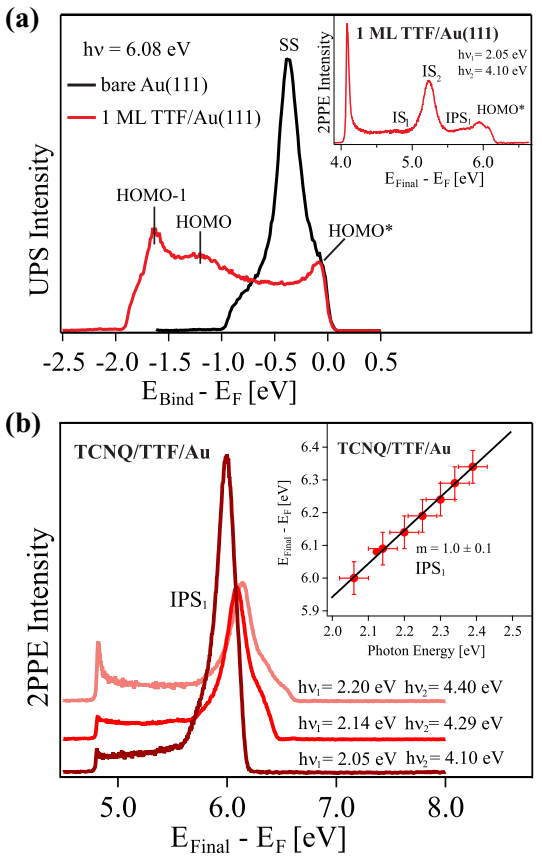

FIG. 3. (a) UPS spectra of the bare and TTF-covered Au(111) surface. For the bare Au(111) the Shockley surface state (SS) is observed, while the state labeled as HOMO* is the result of a hybridization between the SS and the TTF highest occupied molecular orbital. The inset shows a 2PPE spectrum of 1 ML TTF/Au(111) recorded with 2.05 and 4.10 eV photons. Based on photon energy dependent measurements the photoemission peaks labeled as IS_1 and IS_2 can be assigned to TTF-derived unoccupied electronic states located at 2.25 eV (IS_1) and 3.22 eV (IS_2) above E_F. IPS_1 is attributed to the first image potential state located 3.65 eV above E_F (corresponding to 0.5 eV below the vacuum energy). (b) 2PPE data of the mixed TCNQ/TTF/Au(111) monolayer after annealing to 370 K recorded at different photon energies. On the basis of the photon energy dependent 2PPE measurements (see inset) the strong photoemission feature can be assigned to the IPS_1.

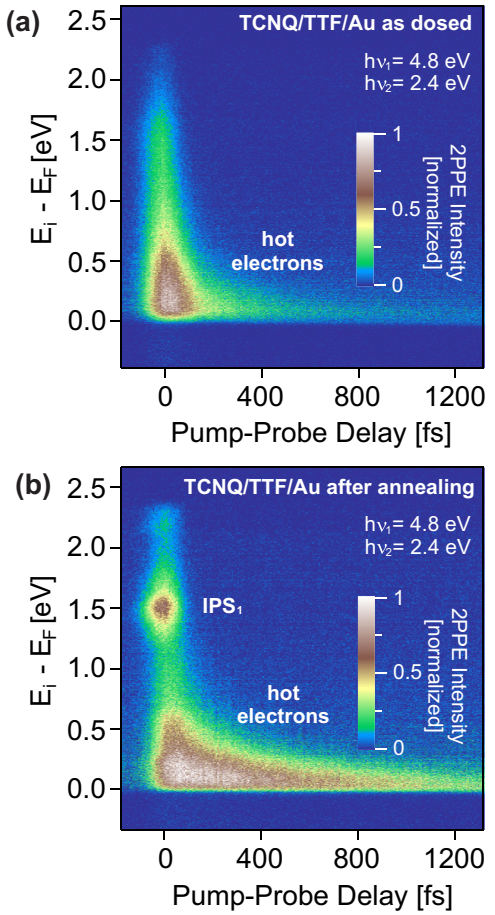

FIG. 4. Hot-electron dynamics at the TCNQ-covered TTF/Au(111) interface. Two-dimensional representations of TR-2PPE measurements for a TCNQ-covered TTF/Au(111) interface with 1 ML coverage (a) before and (b) after annealing up to 370 K.

applied probe photon energy for TR-2PPE measurements has to be increased, in this case up to 4.8 eV. Figure 4(a) shows a two-dimensional representation of TR-2PPE measurements of this TCNQ-covered TTF/Au(111) interface. As can be seen, TCNQ adsorption does not affect the hot-electron dynamics at this interface. However, a subsequent annealing step up to 370 K leads to an increased mobility and intercalation of TCNQ molecules into the TTF layer as it can be traced back via the desorption of nonsurface bound TCNQ and TTF molecules in TPD measurements. The corresponding TR-2PPE measurement for this annealed TCNQ/TTF/Au(111) sample is shown in Fig. 4(b). Surprisingly, TCNQ intercalation induces a significant increase of the hot-electron lifetimes for low intermediate-state energies. Before studying the dynamics in more detail, we investigated the electronic structure of the mixed TCNQ/TTF film using energy-resolved 2PPE as shown in Fig. 3(b). The 2PPE spectra are dominated by one strong photoemission peak. On the basis of photon energy dependent measurements [see also inset of Fig. 3(b)], the peak can be assigned to the first image potential state IPS_1 located 4.0 eV above E_F. Angle-resolved 2PPE data underline this assignment, since the IPS_1 shows a free-electron-like dispersion (data not shown). Using various photon energies no further photoemission features are observed. The comparison between the electronic structure of the TTF/Au(111) interface before and after TCNQ intercalation demonstrates pronounced differences: (i) The work function increases by 650 meV from 4.15 ± 0.04 eV for the TTF/Au(111) to 4.8 ± 0.1 eV for TCNQ/TTF/Au(111). (ii) The HOMO* hybrid state, which has been observed for TTF/Au(111) also with 2PPE [see inset of Fig. 3(a)] is absent in TCNQ/TTF/Au(111). (iii) Unoccupied electronic states assigned to interface states (IS_1 and IS_2) of TTF/Au(111) [see inset of Fig. 3(a)] are not found for TCNQ/TTF/Au(111). We will discuss the influence of the electronic structure changes on the hot-electron dynamics below.

In order to quantify the influence of TCNQ intercalation on the hot-electron dynamics Fig. 5 displays the energy-dependent hot-electron lifetimes before and after the anneal-

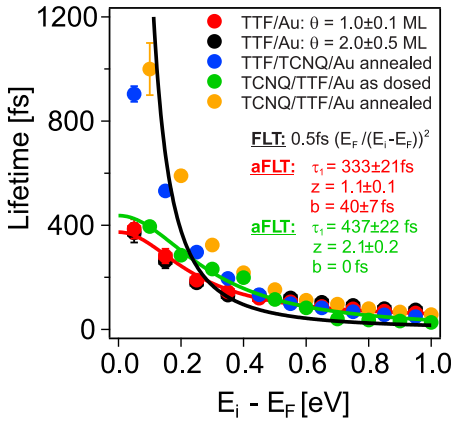

FIG. 5. Comparison of resulting intermediate-state energy dependent hot-electron dynamics. Resulting intermediate state energy dependent hot-electron lifetimes for TTF/Au(111) at different coverages and TCNQ intercalated TTF/Au(111) before and after the annealing step up to 370 K. For comparison, hot-electron dynamics were also investigated for the inverse evaporation sequence: TTF on TCNQ on Au(111) after annealing up to 370 K.

ing, in comparison to our previous findings at the TTF/Au(111) interface for different coverages (1 and 2 MLs). Additionally, the electron dynamics have also been investigated for a sample produced with the inverse evaporation sequence, namely TTF/TCNQ/Au(111). Compared to the TTF/Au(111) interface, dosing TCNQ on top leaves the hot-electron dynamics almost unchanged as it can also be followed by an aFLT fit. In contrast, thermally induced TCNQ intercalation into the TTF layer strongly affects the hot-electron dynamics. Here the lifetimes asymptotically increase for infinitesimal intermediate-state energies as predicted by pure FLT, which suggests a completely electron-electron scattering assisted decay. Consequently, the additional hot-electron relaxation channel formerly observed at the TTF/Au(111) interface is now quenched. This clearly indicates that this additional relaxation channel is not a solid-state phenomenon but rather an interfacial effect, i.e., it cannot be explained by electron-phonon scattering. We believe that electron-electron scattering is the dominant relaxation phenomenon for photoexcited hot electrons at the Au(111) interface in accordance with FLT. The adsorption of alkali metal atoms [19] or even a monolayer of electron-donating molecules such as TTF highly impacts the hot-electron relaxation dynamics at these interfaces, as they donate an additional amount of electrons to the Au(111) surface. In the case of TTF, an electron transfer to the Au(111) surface in combination with hybrid band formation lowers the work function and leads to the formation of an increased density of occupied and unoccupied electronic states near E_F [20–22]. This increased density of states constitutes an increased amount of available scattering partners as well as an increased available phase space resulting in an additional fast electron-electron scattering assisted hot-electron relaxation channel most pronounced visible for low intermediate-state energies at the TTF/Au(111) interface. (Note that the reduction of the lifetime should affect all energies above E_F. Due to the limited experimental temporal resolution it is less evident for higher energies.) The same argumentation is usually applied to explain the shorter hot-electron lifetimes in transition metals, since d-orbitals of transition metals contribute to the electron density of states at and above E_F [5,9,36]. While adsorbing TTF or TCNQ on top of this TTF/Au(111) interface has almost no influence on hot-electron dynamics, the thermally induced TCNQ intercalation leads to a suppression of hybridization between metal and TTF molecular states/bands as can be seen from the photoemission data [see Fig. 3(b)], due to the strong charge-transfer-type intermolecular donor (TTF)/acceptor (TCNQ) interactions [37,38]. Additionally, this is accompanied by a decrease in the density of electronic states near E_F, a decrease in phase space, a decrease in the concentration of appropriate scattering partners, and, in conclusion, an increase of the hot-electron lifetimes. According to FLT, TCNQ intercalation finally triples the hot-electron lifetimes measured for the TTF/Au(111) interface up to about 1000 fs for infinitesimal final-state energies. Thus, this underlines that the additional hot-electron relaxation channel at the TTF/Au(111) interface is related to a pure interfacial effect. Furthermore, we conclude that the hot-electron lifetimes determined at TCNQ/TTF/Au(111) mirrors the lifetimes of hot electrons in bare Au(111).

IV. CONCLUSIONS

In summary, we have performed femtosecond time-resolved two-photon photoemission (TR-2PPE) measurements in order to investigate the influence of adsorbed electron-donating molecules on the hot-electron dynamics at metal surfaces. We found for the tetrathiafulvalene (TTF)-covered Au(111) in the low intermediate-state energy ($E_i - E_F$) regime deviations from Fermi-liquid theory (FLT) leading to hot-electron lifetimes of around 340 fs. Modelling the data with the applied FLT (aFLT) resulted in a second hot-electron relaxation channel, which we assigned to an interfacial phenomenon. Thus, the electron-donating nature of TTF provides an increased density of states near E_F which constitutes an increased amount of available scattering partners as well as an increased available phase space for electron-electron scattering events. This in turn leads to an additional fast electron-electron scattering mediated hot-electron relaxation channel for low intermediate-state energies at the TTF/Au(111) interface. This hot-electron decay channel is most likely also responsible for the ultrafast relaxation in alkali-metal-atom-covered Au(111) surfaces, for which originally an electron-phonon scattering assisted relaxation channel has been proposed. Disturbing the electron donating process and the well-defined electronic landscape by intercalation of electron-accepting tetracyanoquinodimethane (TCNQ) molecules has led to quenching of this second hot-electron relaxation channel. The hot-electron lifetimes asymptotically increased for infinitesimal small intermediate-state energies as predicted by pure FLT. We suggested that this behavior should also be valid for the bare Au(111) surface. As hot-electron dynamics at metal surfaces are crucial for charge transport properties and chemical reactions at metal/organic interfaces this contribution might be a first step in order to understand the influence of adsorbate-induced electronic states on hot-electron dynamics.

ACKNOWLEDGMENTS

Funding by the German Research Foundation (DFG) through the collaborative research center SFB 1249 (Project No. B06) is gratefully acknowledged. D.G. acknowledges financial support from the Heidelberg Graduate School of Fundamental Physics.

[1] S. A. Buntin, L. J. Richter, R. R. Cavanagh, and D. S. King, Phys. Rev. Lett. **61**, 1321 (1988).
[2] X.-Y. Zhu, Annu. Rev. Phys. Chem. **45**, 113 (1994).
[3] F. M. Zimmermann and W. Ho, Surf. Sci. Rep. **22**, 127 (1995).
[4] H. Guo, P. Saalfrank, and T. Seideman, Prog. Surf. Sci. **62**, 239 (1999).
[5] M. Bauer and M. Aeschlimann, J. Electron Spectrosc. Relat. Phenom. **124**, 225 (2002).
[6] H. Nienhaus, Surf. Sci. Rep. **45**, 1 (2002).
[7] G. Schulze, K. J. Franke, and J. I. Pascual, Phys. Rev. Lett. **109**, 026102 (2012).
[8] C. Bronner, B. Priewisch, K. Rück-Braun, and P. Tegeder, J. Phys. Chem. C **117**, 27031 (2013).
[9] M. Bauer, A. Marienfeld, and M. Aeschlimann, Prog. Surf. Sci. **90**, 319 (2015).
[10] M. Aeschlimann, M. Bauer, and S. Pawlik, Chem. Phys. **205**, 127 (1996).
[11] M. Bauer, S. Pawlik, and M. Aeschlimann, *Optoelectronics and High-Power Lasers & Applications* (International Society for Optics and Photonics, San Jose, CA, 1998), pp. 201–210.
[12] E. Knoesel, A. Hotzel, and M. Wolf, Phys. Rev. B **57**, 12812 (1998).
[13] M. Aeschlimann, M. Bauer, S. Pawlik, R. Knorren, G. Bouzerar, and K. H. Bennemann, Appl. Phys. A **71**, 485 (2000).
[14] R. Porath, T. Ohms, M. Scharte, J. Beesley, M. Wessendorf, O. Andreyev, C. Wiemann, and M. Aeschlimann, *Low-Dimensional Systems: Theory, Preparation, and Some Applications* (Springer, New York, 2003), pp. 227–239.
[15] F. Ladstadter, P. F. de Pablos, U. Hohenester, P. Puschnig, C. Ambrosch-Draxl, P. L. de Andres, F. J. García-Vidal, and F. Flores, Phys. Rev. B **68**, 085107 (2003).
[16] M. Lisowski, P. A. Loukakos, U. Bovensiepen, and M. Wolf, Appl. Phys. A **79**, 739 (2004).
[17] A. Goldmann, R. Matzdorf, and F. Theilmann, Surf. Sci. **414**, L932 (1998).
[18] J. J. Quinn and R. A. Ferrell, Phys. Rev. **112**, 812 (1958).
[19] J. Cao, Y. Gao, H. E. Elsayed-Ali, R. J. D. Miller, and D. A. Mantell, Phys. Rev. B **58**, 10948 (1998).
[20] I. Fernandez-Torrente, S. Monturet, K. J. Franke, J. Fraxedas, N. Lorente, and J. I. Pascual, Phys. Rev. Lett. **99**, 176103 (2007).
[21] O. T. Hofmann, G. M. Rangger, and E. Zojer, J. Phys. Chem. C **112**, 20357 (2008).
[22] D. Gerbert, Ph.D. thesis, Ruprecht-Karls-Universität Heidelberg, 2017.
[23] P. Tegeder, J. Phys.: Condens. Matter **24**, 394001 (2012).
[24] E. Varene, L. Bogner, C. Bronner, and P. Tegeder, Phys. Rev. Lett. **109**, 207601 (2012).
[25] L. Bogner, Z. Yang, M. Corso, R. Fitzner, P. Bäuerle, K. J. Franke, J. Pascual, and P. Tegeder, Phys. Chem. Chem. Phys. **17**, 27118 (2015).
[26] L. Bogner, Z. Yang, S. B. M. Corso, R. Fitzner, P. Bäuerle, K. J. Franke, J. Pascual, and P. Tegeder, J. Phys. Chem. C **120**, 27268 (2016).
[27] J. Cao, Y. Gao, R. J. D. Miller, H. E. Elsayed-Ali, and D. A. Mantell, Phys. Rev. B **56**, 1099 (1997).
[28] M. K. Weilmeier, W. H. Rippard, and R. A. Buhrman, Phys. Rev. B **59**, R2521 (1999).
[29] J. Hohlfeld, S.-S. Wellershoff, J. Güdde, U. Conrad, V. Jähnke, and E. Matthias, Chem. Phys. **251**, 237 (2000).
[30] P. Saalfrank, Chem. Rev. **106**, 4116 (2006).
[31] C. Frischkorn and M. Wolf, Chem. Rev. **106**, 4207 (2006).
[32] J. J. Quinn, Appl. Phys. Lett. **2**, 167 (1963).
[33] P. M. Echenique, J. M. Pitarke, E. V. Chulkov, and A. Rubio, Chem. Phys. **251**, 1 (2000).
[34] I. G. Gurtubay, J. M. Pitarke, and P. M. Echenique, Phys. Rev. B **69**, 245106 (2004).
[35] J. Fraxedas, S. Garca-Gil, S. Monturet, N. Lorente, I. Fernández-Torrente, K. J. Franke, J. I. Pascual, A. Vollmer, R.-P. Blum, N. Koch, and P. Ordejón, J. Phys. Chem. C **115**, 18640 (2011).
[36] A. Mönnich, J. Lange, M. Bauer, M. Aeschlimann, I. A. Nechaev, V. P. Zhukov, P. M. Echenique, and E. V. Chulkov, Phys. Rev. B **74**, 035102 (2006).
[37] A. F. Garito and A. J. Heeger, Acc. Chem. Res. **7**, 232 (1974).
[38] A. Della Pia, M. Riello, D. Stassen, T. S. Jones, D. Bonifazi, A. De Vita, and G. Costantini, Nanoscale **8**, 19004 (2016).